Chylomicron remnant uptake is regulated by the expression and function of heparan sulfate proteoglycan in hepatocytes

Bing-Ji Zeng, Bok-Cheng Mortimer, Ian J. Martins, Ulrich Seydel, and Trevor G. Redgrave[1]

Department of Physiology, The University of Western Australia, Nedlands, WA, 6907, Australia

Abstract   Chylomicron remnants transport cholesterol from the intestine, and are removed from the circulation principally by the liver. While hepatic receptors, including the low density lipoprotein (LDL) receptor account for endocytosis, heparan sulfate proteoglycans (HSPG) participate in the initial binding of remnants to liver cells. To explore the interactions between HSPG and endocytosis of remnants, in the present study the expression of HSPG was inhibited in HepG2 cells transfected by a synthetic antisense oligodeoxynucleotide SYN5. Immunofluorescent staining by a monoclonal anti-syndecan antibody showed significant reduction in the expression of syndecan in SYN5-treated cells compared with control cells. Remnant binding decreased by about 50–70% in SYN5-transfected cells. Monoclonal antibodies to either heparan sulphate or the LDL receptor decreased binding by about 60–65%. The glycosylation inhibitor β-nitrophenyl-xylopyranoside inhibited remnant uptake by 25%, whereas 4-nitrophenyl-β-d-galactopyranoside had no effect on remnant binding. Heparinase completely abolished binding at appropriate concentrations. Heparitinase was less effective than heparinase in inhibiting remnant binding. Suramin completely abolished the remnant binding. Poly-arginine, poly-lysine, and protamine all reduced remnant uptake by the cells, as did polybrene, a synthetic polycation, suggesting a role of cation–anion interactions in remnant binding. Brefeldin A, colchicine, and monensin caused the fluorescence associated with remnants to persist within the cells, confirming that blockers of tubulovesicular processes and Golgi function inhibit the intracellular transport and degradation of the remnants.   Our results show that remnant binding to liver cells depends on the LDL receptor, on the expression of HSPG core proteins, and on the functionality of heparan sulfate in HSPG.—**Zeng, B-J., B-C. Mortimer, I. J. Martins, U. Seydel, and T. G. Redgrave.** Chylomicron remnant uptake is regulated by the expression and function of heparan sulfate proteoglycan in hepatocytes. *J. Lipid Res.* 1998. **39:** 845–860.

Supplementary key words   antisense • antibody • competitor • inhibitor • receptor • blocker • metabolism • lipoprotein • glycosaminoglycan • confocal microscope

The two-step process of chylomicron catabolism includes lipolysis by lipoprotein lipase to form remnants and the subsequent clearance of remnants by receptor-mediated uptake in the liver. The detailed mechanism of the receptor-mediated uptake of remnants in the liver is yet unclear and the receptors involved in recognition of chylomicron remnants remain controversial (1, 2).

Using gene knockout mice deficient in apolipoprotein (apo)E or deficient in low density lipoprotein (LDL) receptor, we recently showed that apoE and LDL receptors are both essential for the normal, fast clearance of chylomicron remnants by the liver (3). In the absence of LDL receptors, as alternative apoE-dependent pathway operates to clear the chylomicrons from the plasma, with significantly delayed catabolism. Nevertheless, the alternative pathway of hepatic remnant uptake is sufficient to prevent the LDL receptor-deficient mice from accumulating apoB48-containing lipoproteins in the circulation. This pathway probably also explains the observations that chylomicron remnants are not accumulated in the plasma of WHHL rabbits (4) or in patients with familial hypercholesterolemia (5). The receptor involved in this pathway has not been identified, although the LDL receptor-related protein (LRP), the asialoglycoprotein receptor (6), and the lipolysis-stimulated receptor (LSR) (7) have been suggested.

In normal and LDL receptor-deficient mice, plasma clearance and hepatic uptake of chylomicron remnants were enhanced by the presence of soluble heparin and

inhibited by suramin and lactoferrin, which interfere with the function of heparan sulfate proteoglycan (HSPG) (8, 9). Remnant uptake by liver cells in intact mice and in tissue culture was also retarded by heparinase, which degrades the polysaccharide chains on HSPG (10, 11). Moreover, mutant CHO cell lines deficient in HSPG demonstrated a reduced uptake of remnants (12). On the basis of evidence that heparan sulfate was involved in the uptake process of remnants by the liver, Ji et al. (13) postulated an initial sequestration of remnant particles within the space of Disse through interaction with HSPGs on the surface of hepatocytes.

HSPGs are polyanionic macromolecules that contain a protein core with multiple heparan sulfate chains covalently attached. The biological roles of HSPGs relate to the binding of ligands to heparan sulfate chains. However, biological activity also depends to some extent on the core protein (14), which assumes anchoring function and provides a scaffold for appropriate immobilization and spacing of the heparan sulfate chains. In the liver, the major core proteins are the syndecans, although glypican, betaglycan, and perlecans (15) are also present. Syndecans are a family of cell surface heparan sulfate proteoglycans, which consists of four distinct members in mammals, designated as syndecans 1–4 (or syndecan, fibroglycan, N-syndecan, and amphiglycan, respectively). Although the functions of the syndecan family are not known in detail, they are believed to play important roles in morphogenesis and differentiation by binding to a variety of extracellular ligands. Most of the proposed functions of syndecans are related to their ability to recognize extracellular effector molecules. Syndecan-1, a prototype of integral membrane heparan sulfate proteoglycans, is the first well-characterized member of this protein family. The core protein of syndecan-1 contains about 80% of heparan sulfate in mouse mammary epithelial cells (16). In hepatocytes, HSPGs are thought to bridge the extracellular matrix and the intracellular cytoskeleton, whereas HSPGs bound to endothelial cell plasma membranes facilitate the binding of circulating macromolecules including growth factors, lipoprotein lipase, and probably lipoproteins and remnants.

While growing evidence indicates the involvement of heparan sulfate chains in hepatic remnant uptake, it is not known whether the core proteins of cell surface HSPG (15) contribute to the process of hepatic remnant uptake. The present study was undertaken to investigate the effects on remnant uptake of decreased syndecan expression. In addition, we explored the relative contributions of HSPG and LDL receptors and their interactions in remnant uptake.

EXPERIMENTAL PROCEDURES

Animals and materials

Male Wistar rats were obtained from the Animal Resource Centre, Murdoch, Western Australia. Egg yolk phosphatidylcholine was purchased from Lipid Products (Surrey, UK). Cholesterol, cholesteryl oleate, and triolein were from Nu-Chek-Prep. (Elysian, MN). The fluorescent probe, cholesteryl-4,4-difluoro-5,7-dimethyl-4-bora-3α4α-diaza-s-indacene-3-dodecanoate (BODIPY-CE) was purchased from Molecular Probes Inc. (Eugene, OR). Anti-low density lipoprotein receptor monoclonal antibody (clone C7) and [^{35}S]sodium sulfate (carrier-free) was obtained from Amersham (New South Wales, Australia). Radioactivity was counted by a liquid scintillation counter (Beckman). Anti-heparan sulfate monoclonal antibody, 10E4, was purchased from Sapphire Bioscience (New South Wales, Australia). Suramin was from Bayer (Australia). Anti-syndecan IgG from rat and FITC-labeled mouse anti-rat IgG were purchased from PharMingen (San Diego, CA). Brefeldin A, monensin, colchicine, heparinase I (EC 4.2.2.7), and heparitinase I (EC 4.2.2.8), polyinosinic acid, and fucoidan were from Sigma. The liposomal transfection reagent N-[1-(2,3-dioleoyloxy)propyl]-N,N,N-trimethylammonium methyl sulfate (DOTAP) was from Boehringer Mannheim, and 4-nitrophenyl-β-d-xylopyranoside and 4-nitrophenyl-β-d-galactopyranoside were from Fluka.

Preparation and verification of fluorescently labeled chylomicron-like lipid emulsions

Chylomicron-like lipid emulsions, with and without the fluorescent label BODIPY-CE (0.4 mg per emulsion mixture), were prepared by sonicating a mixture of pure triolein (TO), cholesteryl oleate (CO), egg lecithin, and free cholesterol in 0.154 m NaCl, 10 mm HEPES (pH 7.4). Chylomicron-size particles of diameter 130–150 nm were purified from the sonicated mixture by serial ultracentrifugation in a density gradient. Details of the procedures and characterization of the emulsion particles have been given previously (17).

Plasma clearance studies were performed to verify whether the metabolism of the emulsion was affected by the presence of the fluorescent dye. Emulsions with and without the fluorescent ester were radiolabeled with [^{14}C]triolein and [^{3}H]cholesteryl oleate to trace the lipolysis and remnant removal of the emulsions, respectively. Non-fasted rats were anesthetized and surgically prepared with in-dwelling carotid and venous cannulas as described earlier (17). Briefly, a saline-filled Teflon cannula 0.76 mm o.d. × 0.33 mm i.d. (Small Parts Inc.) was inserted through the left common carotid artery so that the tip was located in the aortic

arch, and a venous cannula 0.8 mm o.d. × 0.5 mm i.d. (Dural, NSW, Australia) was inserted near the junction of the left jugular and subclavian veins. The tip was advanced to lie in the superior vena cava. Heparin was not used but clotting was prevented by treatment of the tubing with Aquasil™ (Pierce, Rockford, IL) before use. After surgery, the animals recovered from the anesthesia in individual restraint cages for 2–4 h before the injection study commenced. The emulsions were injected into the venous cannula as a bolus of ~3 mg lipid in a volume of ~0.5 ml. Blood samples of 0.35 ml were then taken at 3, 5, 8, 12, 20, 25, and 30 min. Each withdrawal was replaced with an equal volume of 0.15 m NaCl. After the final blood sample, a lethal dose of Nembutal was injected. The liver and spleen were excised for extraction of radioactive lipid from minced whole spleen and from minced 1-g pieces of weighed liver. Lipids were extracted into 30 ml of chloroform–methanol mixture 2:1 (v/v), then aliquots were taken, the solvent was evaporated, and radioactivity was measured by liquid scintillation spectrometry. Radioactivity in plasma was measured, without extraction, in 150-μl samples using Emulsifier-safe™ (Packard). Plasma clearance kinetics were computed as fractional clearance rates from the mono-exponential curves fitted by least squares procedures to samples taken during the first 12 min after injection. The plasma clearance and organ uptakes of [^{3}H]cholesteryl oleate and [^{14}C]triolein in emulsions with and without the fluorescent cholesteryl ester were similar (results not shown).

Preparation and evaluation of fluorescently labeled chylomicron remnants

Fluorescently labeled and non-labeled remnants were prepared using an in vivo method as we have previously described (3, 18). Briefly, approximately 10–15 mg of emulsion–triacylglycerol was injected into functionally hepatectomized rats and allowed to circulate for 30 min. Rats were bled and remnants were then isolated by density-gradient ultracentrifugation from the plasma. Chylomicron remnants were stored in the dark under argon with reduced glutathione (Sigma, 50 μg/mL) to prevent lipid oxidation and were used within 24 h of preparation. The amount of remnant proteins added to the cells was 15.1 ± 2.8 μg/ml (n = 14).

Fluorescently labeled remnants were cleared from the plasma in the same way as normal remnants. The in vivo metabolism of the fluorescently labeled remnants was evaluated by examining the confocal images of liver sections from rats injected with the remnant lipoproteins. Aliquots of remnants were injected via the jugular vein of anesthetized rats. Ice-cold saline was perfused through the portal vein at 1, 5, 10, and 30 min after injection and the liver was excised. Liver pieces

(3–4 mm^3) were placed in 4% paraformaldehyde in 0.1 m cacodylate buffer overnight, snap frozen with isopentane in liquid nitrogen, and sectioned on a cryostat (Bright, UK). Sections were collected on gelatin-coated slides, mounted in an aqueous medium, and examined by a Bio-Rad MRC-1000 confocal laser scanning fluorescent microscope with lens, Plan Apo 40X, NA 1.40 (Bio-Rad Microscience, Hemel Hempstead, UK).

Preparation of remnant-like emulsion particles

Remnant-like emulsions were prepared by sonication and purified by ultracentrifugation as previously described (19). The emulsions were prepared from mixtures of TO (4.5 mg), phosphatidyl choline (PC) (2.5 mg), CO (0.5 mg), and cholesterol (0.8 mg). For preparation of the fluorescently labeled particles, 0.1 mg of a fluorescent probe, BODIPY-CE, purchased from Molecular Probes (Eugene, OR), was added. After a 1 h sonication of the lipid mixture in 8.5 ml of 2.2% glycerol in water, the crude emulsion was placed at the bottom of two centrifuge tubes, and then 2.5 ml of NaCl solutions of densities 1.065, 1.040, and 1.020 g/ml were sequentially layered above. The tubes were then centrifuged in a SW 41 rotor of a Beckman L8-70M ultracentrifuge for 60 min at 30,000 rpm and 20°C. The particles that floated to the surface were removed and used for cell culture studies. The remnant-like emulsion particles were of average diameter 73 ± 7 nm (n = 30) measured by negative-stain electron microscopy.

Binding of apoE3 to remnant-like emulsions

Remnant-like emulsions (100 μl) were mixed with 10 μg of human recombinant apoE3 (Pan Vera Corp., Madison, WI). The emulsion–apoE3 mixture was sonicated three times for 1 sec with a 2-sec interval between each sonication pulse using a Sonic and Material Inc. microtip (Danbury, CT).

Cell culture

HepG2 and McA-RH7777 cells were obtained from ATCC. The cells were cultured at 37°C in a 25-mL flask (Corning, NY) containing 5 mL of Eagle's minimal essential medium (MEM) (Flow Lab., Australia) supplemented with 10% fetal calf serum (FCS) (Flow Lab., Australia), plus 2 mm glutamine (Merck), plus antibiotics (100 units/ml penicillin, Calbiochem, La Jolla, CA and 100 μg/ml streptomycin, Calbiochem) under 5% CO_2/95% air incubator (Hepa Filtered, IR Incubator, Forma Scientific, Marietta, OH). Doubling time of the cells was approximately 16 h. The medium was renewed twice a week. Confluent cultures were subcultured using a split ratio of 1:10. For the binding experiment stock cells were detached when confluent using

0.025% (w/v) trypsin/EDTA in Hank's balanced salt solution (BSS), diluted with appropriate media, and plated on coverslips in 35-mm plastic culture dishes (Disposable Products, Australia). The cells were used when they were near confluence (~70%).

Synthesis of oligodeoxynucleotides and in vitro transfection

Oligodeoxynucleotides (ODNs) and phosphorothioate ODNs were synthesized and sequenced by Biotech International Ltd. (Bentley, Australia). The sequences of ODNs used were as follows: antisense SYN5 (5′-GCGGGTTCCGCTGCTCGATG-3′) complementary to nucleotides −82 to −63 of the human syndecan-1 gene and sense sequence (5′-CATCGAGCAG CGGAACCCGC-3′) (20). In designing ODNs, we avoided the four contiguous guanosine residues (the 4G) and the 2 × 3G sequences that have been reported to produce sequence specific but nonantisense effects (21). Additional control studies were performed with sense (+1766 to +1785 nucleotides of the human syndecan cDNA consisting of 5′-AGCATCAG GGTTAAGAAGAC-3′) and the antisense ODN complementary to this sequence. Oligodeoxynucleotides were complexed to DOTAP (Boehringer Mannheim) before adding to cells (final concentrations of 0.5 and 1 nm) at the time of cell plating. The cells were then incubated for 24 or 48 h at 37°C. To measure binding, control cells and cells transfected with antisense ODN, sense ODN, or with DOTAP only were washed 3 times with prewarmed MEM and kept in MEM at 37°C for 2 h. An aliquot of 50 μl fluorescent labeled remnants in fresh medium was then added to the cells and incubated for 5 min. Cells were washed and subsequently equilibrated with non-labeled remnants as described above.

Immuno-fluorescent staining of syndecan expression in HepG2 cells

Cells were cultured for 24 h in 35-mm dishes (10^6 cell/ml per dish) containing antisense or sense ODN (1 nm) in DOTAP. Rat anti-syndecan IgG (15 μg/ml per dish) was added to the cells.

After an overnight incubation, the cells were washed 3 times with BSS before the addition of FITC-labeled mouse anti-rat IgG (30 μg/ml per dish) in MEM and kept at 37°C for 2 h. After incubation cells were washed 5 times with warm BSS and then fixed for confocal microscopic examination as described above.

Incorporation of [^{35}S]sulfate in HepG2 cells

Cells were labeled according to Rapraeger and Bernfield (22) with slight modifications. Cells cultured in 35-mm dishes (10^6 cell/ml per dish) containing antisense or sense oligonucleotides in the liposome DOTAP, or DOTAP only were radiolabeled for 48 h by adding 50 μCi/ml [^{35}S]sulfate in MgSO$_4$-free MEM (10% FCS) at the time of the cell plating. The medium was removed and cells were washed twice with BSS. An aliquot of 0.6 ml trypsin solution (0.05%) containing 0.02% EDTA was added to the cells and incubated for 10 min at 20°C. After centrifugation, the supernatant was aspirated into a fresh tube and cells were resuspended in 0.6 ml BSS. Cells were pelleted at 13,000 rpm for 5 min and the supernatants were combined and measured for labeled material released from the cell surface (22). The cell pellets were dissolved in 1 ml SDS solution (1%) overnight at 20°C to quantify the labeled material remaining with the cells by scintillation counting.

Binding and uptake studies

A pulse-chase design was used to study the binding and uptake of fluorescent remnants. An aliquot of 50 μl of fluorescent labeled remnants were added and incubated for 5 min at 37°C. At the end of the incubation, cells were washed 5 times with BSS (37°C) and then incubated with equal amount of non-labeled remnants for 1, 10, 30, or 50 min. Cells were then fixed with 4% paraformaldehyde in 0.1 m cacodylate buffer for 10 min at 4°C. The cover slips were removed from the culture dish and mounted on slides with Aquamont for examination by a Bio-Rad MRC-1000 confocal scanning microscope with lens, Plan Apo 60×, NA 1.40.

In the present study binding refers to fluorescent remnants bound to the cell surface after pulse-chase 5 min and equilibrium with non-labeled remnants at 37°C. Uptake refers to internalization of remnants bound by the cells. Optical sectioning (Z-series) was used to distinguish between bound and internalized remnants. The fluorescent signal with the cells was very low compared to surface labeling when cells were scanned after 5 min incubation with fluorescently labeled remnants followed by incubation for 1 min with unlabeled remnants. The pixel number and intensity were similar to the experiments done at 4°C (results not shown), suggesting that uptake is negligible at this time point. Only after 10 min incubation with unlabeled remnants was the fluorescent signal visualized within the cells, indicating internalization of remnants by the cells.

The cells were incubated with various competitors or inhibitors at indicated concentrations at 37°C for 1 h in FCS-deficient MEM. In other experiments, solutions containing a monoclonal antibody to heparan sulfate, heparinase, or heparitinase were added to the cells before incubation at 37°C for 24 h. Cells incubated with an-

tibody were washed 3 times with warm MEM to reduce the non-specific binding and kept in 1 ml MEM at 37°C for 1 h prior to the binding studies as described above.

For the experiments of remnant-like emulsion binding, cells incubated with rat anti-syndecan IgG, monoclonal anti-LDL receptor IgG, or both antibodies at 37°C for 2 h after transfection with antisense or sense ODNs complexed with DOTAP, followed by three washes with 1 ml of cold BSS. Cells were incubated in 1 ml of cold MEM with fluorescently labeled remnant-like emulsions at 4°C for 30 min. After incubation cells were washed 5 times with cold BSS and then fixed for confocal microscopic examination as described above.

Chemical analysis

Lipid phosphorus was measured by the method of Bartlett (23). The lipids extracted from remnants with chloroform–methanol 2:1 (vol/vol) were separated by thin-layer chromatography. Triglyceride (TG) was quantified as glycerol by chromotropic acid (24); free and esterified cholesterol were assayed by the *o*-phthaldialdehyde procedure (25) after saponification of lipids in the separated bands. Protein was assayed by the procedure of Lowry et al. (26).

Analysis of remnant apolipoproteins

Remnant apolipoproteins were separated by sodium dodecyl sulfate polyacrylamide gel (SDS/PAGE) with a gradient of 5–25% polyacrylamide gel. Remnants were partially delipidated by mixing 0.1 ml of sample with 0.6 ml of diethyl ether before they were loaded on to the gel. Bands were stained by Coomassie Blue R-250 (Bio-Rad) and the apolipoproteins were identified by comparison with molecular weight markers.

Statistics

Group means were compared by analysis of variance. Statistical significance was accepted with $P < 0.05$.

RESULTS

Lipid composition and apolipoprotein profile of fluorescently labeled emulsion remnants

The emulsion particles were protein-free when injected, but apolipoproteins, mostly apolipoproteins E and C, became associated with remnants after circulation for 30 min. **Table 1** shows the lipid compositions of fluorescently labeled emulsion remnants, remnant-like emulsions, and lymph chylomicron remnants. The content of cholesterol was less and total protein was more in lymph remnants when compared with emulsion remnants. The remnant-like emulsion contained more PL and less CO when compared with emulsion remnants. **Figure 1** shows that the patterns of apolipoproteins in remnant particles derived from fluorescently labeled emulsions are similar to that derived from the lymph chylomicrons. The presence of apoB-48 and B-100 in the samples of emulsion remnants was possibly related to the presence of endogenous lipoproteins in the plasma of hepatectomized rats.
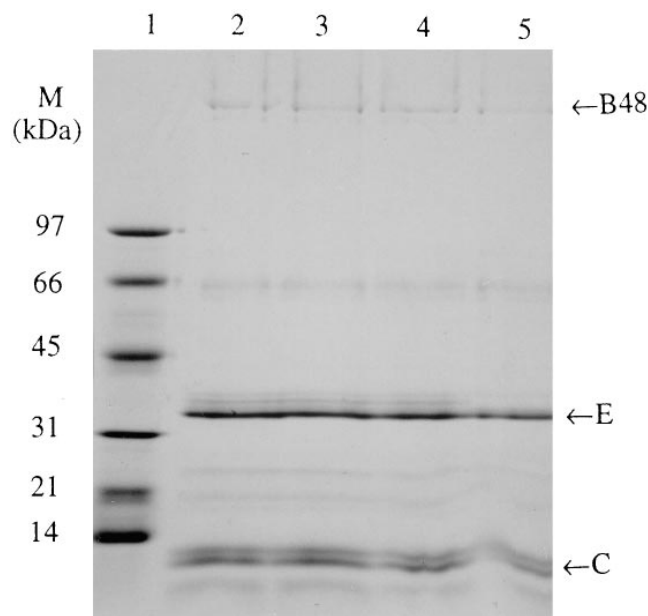
Evaluation of fluorescently labeled remnants in the liver of rats

Figure 2 shows the patterns of remnant uptake and metabolism in the liver at 1 (panel A), 5 (panel B), 10 (panel C), and 30 min (panel D) after intravenous injection into intact rats. Remnants became associated with hepatocytes as early as 1 min after injection, as indicated by the presence of fluorescence on the cell surface. At 5 and 10 min after injection, the increased fluorescent intensity within the cells suggested that more remnants had been internalized and accumulated in the hepatocytes. At 30 min, the fluorescent intensity decreased suggesting that most of the remnants had been metabolized into undetectable products. These results suggest that the fluorescently labeled remnants were metabolized in the same way as the normal remnants.

TABLE 1. Lipid compositions of fluorescently labeled emulsion remnants, remnant-like emulsions, and lymph chylomicron remnants

	Percentage by Weight of Total Lipids				
	TO/TG	CO/CE	PL/PC	FC	Total Protein
Emulsion remnants	52.6 ± 1.9	17.2 ± 2.1	10.7 ± 2.0	9.6 ± 0.9	9.9 ± 1.2
Lymph remnants	64.3 ± 0.9	4.1 ± 0.5	10.7 ± 0.8	3.6 ± 0.5	17.3 ± 0.4
Remnant-like emulsion	58.3 ± 1.3	6.9 ± 0.6	26.4 ± 1.8	8.4 ± 0.7	

Results for TO or triglycerides (TG), CO or cholesteryl esters (CE), phospholipids (PL), phosphatidylcholine (PC), unesterified cholesterol (FC), and total protein are given as mean ± SEM, n = 4 in each group.

Fig. 1. Distribution of apolipoproteins associated with remnants derived from lymph chylomicrons and fluorescently labeled emulsions by gradient SDS/5–25%-PAGE. Remnants were harvested from the plasma of functionally hepatectomized rats injected with lymph chylomicrons or labeled emulsions. Lane 1 contains low-molecular-weight markers; lanes 2 and 3 contain lymph remnant protein (40 μg); lanes 4 and 5 contain fluorescently labeled emulsion remnant protein (40 μg).

Effect of antisense ODN transfection on the de novo HSPG expression and remnant binding

To determine whether decreased expression of syndecan had any effect on remnant binding, cells were transfected with antisense and sense ODNs complexed with DOTAP, incubated with fluorescent labeled remnants at 37°C for 5 min, and re-equilibrated with non-labeled remnants for 1 min. An ODN, named SYN5, 5′-GCGGGTTCCGCTGCTCGATG-3′ complementary to the sequence −82 to −63 upstream to the initiation site of the cDNA reduced remnant binding effectively. Remnant binding was not completely inhibited and a small amount of remnants was internalized. The confocal images in **Fig. 3A** and **B** compare the quantity of binding and uptake of remnants in cells transfected with antisense or the control sense ODNs for 24 h. Remnants bound to cell surface (**Fig. 4**) were quantified by the number of pixels/cell at 1 min equilibration time with non-labeled remnants after the initial incubation with fluorescent remnants as described in Methods. Remnant binding in cells transfected with antisense ODN in different concentrations decreased by 50–70% compared with control cells transfected with the sense ODN at the same concentration or with

DOTAP only (Fig. 4). DOTAP, being a cationic liposome, probably interfered electrostatically to reduce remnant binding by about 15% (see Discussion). However, the effect of DOTAP alone was slight compared with the effect of the antisense ODN SYN5 (Fig. 4). The effect produced by the sense ODN in DOTAP was not different from that of DOTAP alone. Additional controls using antisense and sense ODNs from a less specific region of the syndecan gene showed no effects on remnant binding (results not shown). Results of remnant binding studies obtained from cells after 48 h incubation with the ODNs were similar to the above.

### Reduced expression of syndecan-1 by antisense oligonucleotide SYN5

The effect of the antisense oligonucleotide SYN5 and its sense counterpart, SYN3, (5′-CATCGAGCAGCG GAACCCGC-3′) on the expression of syndecan was compared by using immunofluorescent staining of the protein with an anti-syndecan IgG and by the incorporation of radioactive sulfate into surface and intracellular proteoglycans according to Rapraeger and Bernfield (22). Results from the immunofluorescent staining are shown in **Fig. 5**. Control cells transfected with sense ODN SYN3 expressed large quantities of syndecan as indicated by the fluorescent label of the antibody (Fig. 5C). In contrast, little fluorescence was observed in cells transfected with the antisense ODN SYN5, indicating that the expression of syndecan was much reduced (Fig. 5D).

The reduced expression of syndecan by antisense gene inhibition was confirmed by the sulfate incorporation experiments. Cells were labeled with [^{35}S]sodium sulfate (50 μCi) at the time of cell plating in the presence of antisense and sense ODNs (1.0 nm) in DOTAP (final concentration, 10 μg/ml) and the incorporation [^{35}S]sulfate into cell surface proteoglycans was quantified by scintillation counting of the medium after treatment with trypsin (22). Results showed that ^{35}SO$_4$-labeled sulfated compounds (including heparan sulfate, chrondroitin sulfate, and probably other SO$_4$-containing molecules) on the surface of cells transfected with antisense ODN decreased to 78.3 ± 4.5% (n = 3) compared with controls treated with sense ODN or with DOTAP only. A small portion of intracellular radioactivity was recovered from the cell pellets solubilized in SDS, with no significant difference of ^{35}SO$_4$-labeled cell sulfated compounds between cells treated with sense or antisense ODNs.

Effect of syndecan on LDL receptor-mediated binding of remnants

To characterize whether the binding of remnant-like emulsions was dependent on the function of syndecan
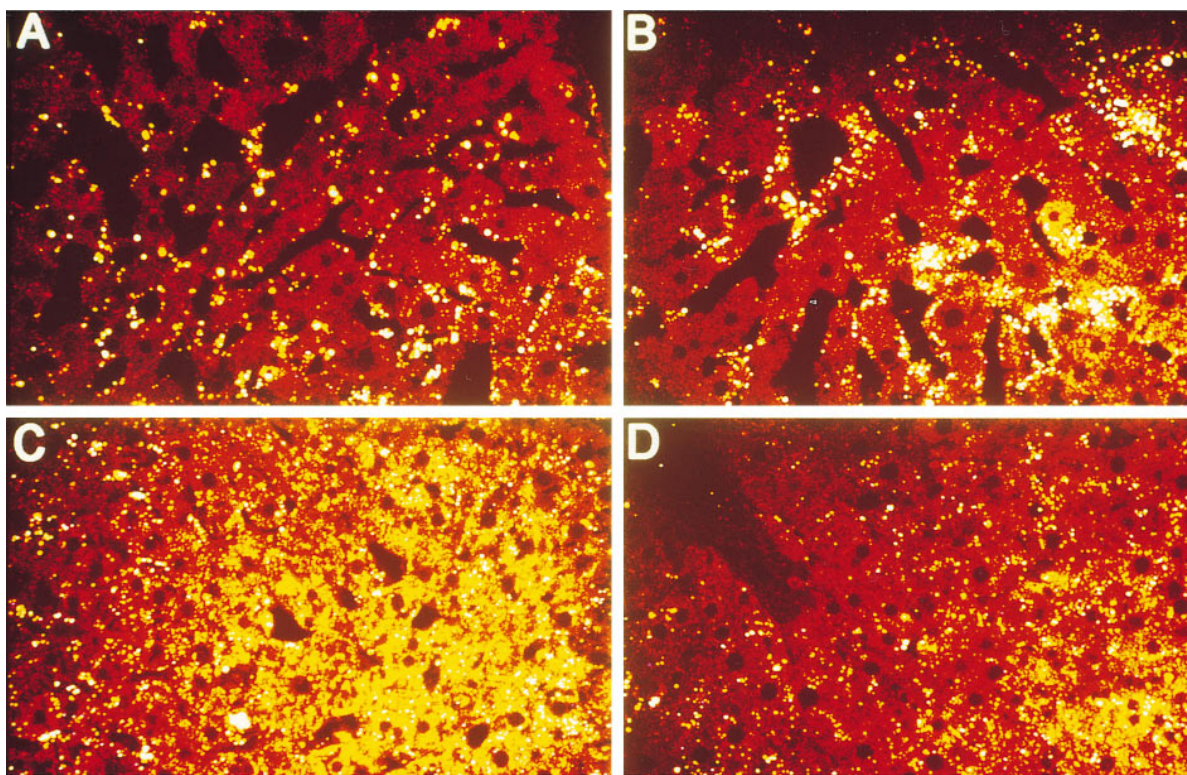
Fig. 2. Uptake and localization of fluorescently labeled chylomicron remnants in liver sections from rats. Remnants were injected intravenously into anesthetized rats and liver pieces were processed for confocal microscopy at 1, 5, 10, and 30 min after injection, as described in the Methods. (A) Binding of remnants to liver cells at 1 min after injection, (B) remnants bound to cell surface and were internalized into the hepatocytes at 5 min, (C) increased fluorescent intensity in hepatocytes indicating continual internalization of remnants at 10 min after injection, and (D) decreased fluorescent intensity at 30 min, suggesting that remnants have been metabolized.

or on the LDL receptor, or both, cells wre transfected with antisense or sense ODNs complexed with DOTAP, incubated with rat anti-syndecan IgG (15 µg/ml), monoclonal anti-LDL receptor IgG (28 µg/ml), or both antibodies at 37°C for 2 h. The cells were then incubated in 1 ml of cold MEM with fluorescently labeled remnant-like emulsions at 4°C for 30 min.

Remnant binding in cells incubated with either the anti-syndecan IgG or the anti-LDL receptor IgG was inhibited highly significantly ($P < 0.001$) but not completely as shown in **Table 2**, indicating that the remnant binding was dependent on both the LDL receptor and the expression of syndecan. Remnants bound to the cell surface were quantified by the number of pixels/cell as shown in Table 2. In cells transfected by sense ODNs, remnant binding was reduced by 51% in anti-syndecan IgG-treated cells and by 61% in anti-LDL receptor IgG-treated cells compared with non-antibody-treated cells ($P < 0.001$). In cells transfected with sense ODNs, remnant binding was reduced by 64% when incubated with both antibodies ($P < 0.001$).

In cells transfected with antisense ODNs, remnant binding was reduced by 67% compared with the control sense-transfected cells ($P < 0.001$). In cells transfected with antisense ODNs, remnant binding was reduced by 75% after incubation with anti-syndecan IgG and by 78% after incubation with anti-LDL receptor IgG when compared with the control sense ODNs-transfected cells without any antibody treatment ($P < 0.001$). In cells transfected with antisense, remnant binding was reduced by 80% after incubation with both antibodies ($P < 0.001$).

Effects of functional inhibitors on remnant binding

The effect of various enzymes, competitors, and inhibitors of heparan sulfate, and membrane transport blockers on remnant binding is shown by the confocal images in **Figs. 6A** and **B**. The enzymes heparinase and heparitinase have been shown to cleave heparan sulfates on HSPG. Heparinase acts upon glucosaminido–iduronic acid linkages where the glucosamine is sulfated at the 2-position while heparitinase is specific for
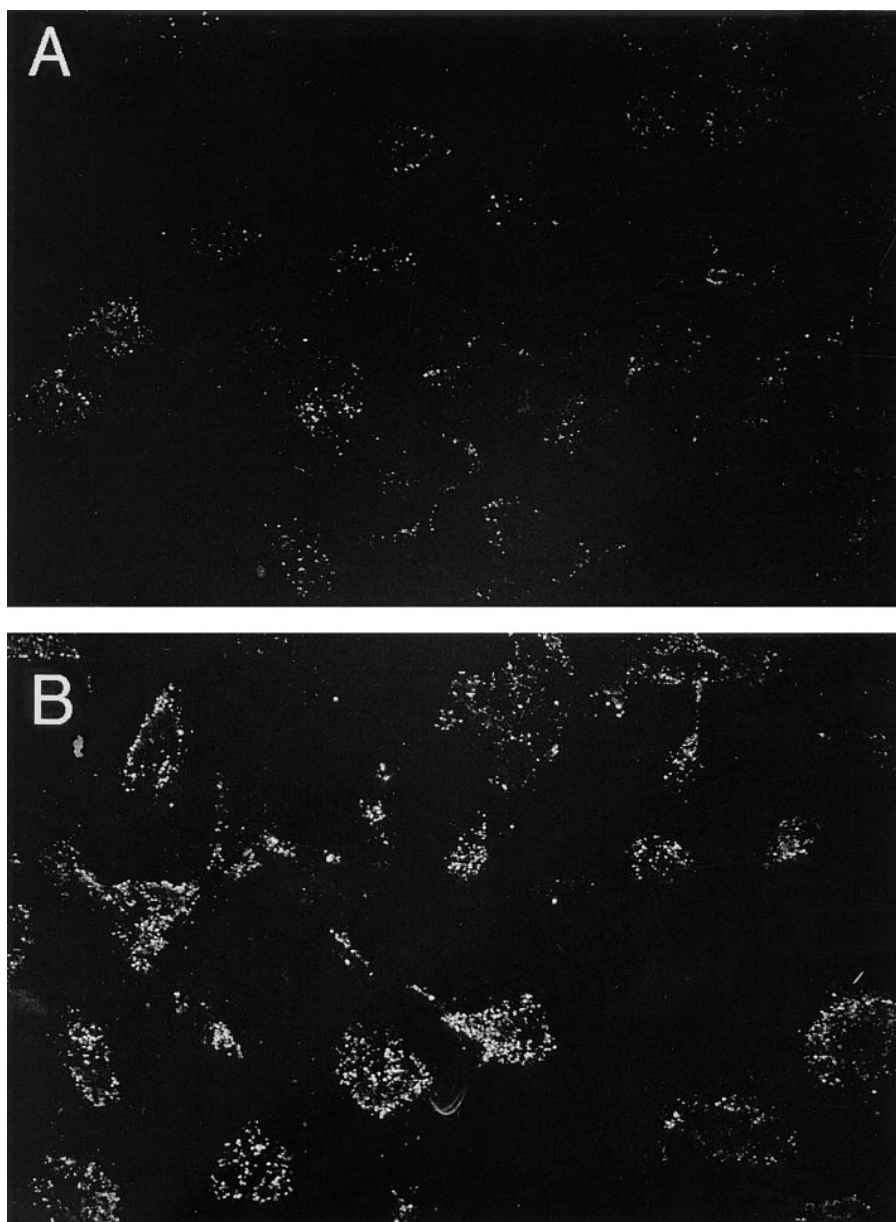
Fig. 3. Uptake of fluorescently labeled chylomicron remnants by non-transfected and transfected HepG2 cells. The cells were transfected with (A) antisense deoxyoligonucleotide (ODN) SYN5 and, (B) sense ODN from −82 to −63 nucleotides of the human syndecan-1 gene, complexed with DOTAP and incubated at 37°C for 24 h. Cells were washed 3 times with MEM and incubated with fresh medium at 37°C for 2 h. An aliquot of 50 μl cholesteryl-BODIPY labeled remnants was added and incubated for an additional 5 min. Cells were washed 5 times with BSS and re-equilibrated with similar amount of non-labeled remnants for 1 min and fixed in 4% paraformaldehyde for 1–2 h. Cells were enlarged 600 times.

N-acetyl or N-sulfate glucosaminido–glucuronic acid linkages (27). Heparinase at 2 units/ml inhibited remnant binding completely, whilst at a lower concentration (1 unit/ml), about 30% of remnant binding remained (Fig. 6). Because of its specificity, lower doses of heparitinase (0.02–0.5 unit/ml) were used and remnant binding was reduced to 77% of control values.

A monoclonal antibody to heparan sulfate (4 ng/ml) reduced remnant binding by 65% when compared with control values. A heparan sulfate synthesis inhibitor, 4-NP-β-d-xylopyranoside (1 mm) (28) reduced remnant binding by 25%, while its analogue, 4-NP-β-d-galactopyranoside had no effect on remnant binding. Suramin (500 μg/ml) blocked remnant binding completely. Fu-
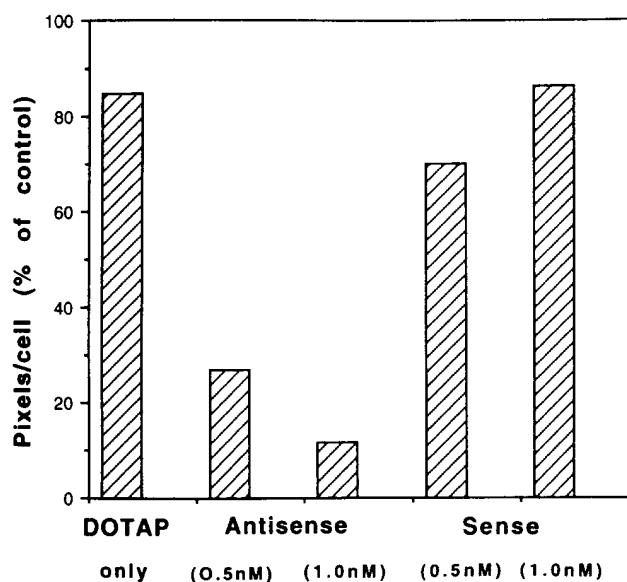
Fig. 4. Effect of antisense and sense transfection on remnants bound to the surface of HepG2 cells. Control cells were incubated with medium only, while tested cells were incubated with sense or antisense oligonucleotides complexed with DOTAP, or DOTAP, only for 24 h, incubated with fresh medium at 37°C for 2 h and then with cholesteryl-BODIPY labeled remnants for an additional 5 min. Cells were washed and re-equilibrated with a similar amount of non-labeled remnants for 1 min and fixed in 4% paraformaldehyde for 1–2 h. Remnants bound to cells were quantified by the fluorescence associated with each cell as number of pixels/cell and expressed as % control value.

coidan (100 μg/ml) also reduced remnant binding effectively (results not shown). The highly positive charged polypeptides, including poly-arginine, poly-lysine and protamine, all reduced remnant binding effectively (data not shown).

Compared with control cells incubated with medium only, remnant binding was not significantly affected in cells pre-treated with low concentrations of membrane transport blockers colchicine (200 μg/ml), brefeldin A (1 μg/ml), monensin (0.7 μg/ml), and polybrene (12.5 μg/ml), $P > 0.05$. However, remnant binding was reduced significantly when higher doses of the drugs (colchicine $\geq$40 μg/ml, brefeldin A $\geq$2.5 μg/ml, monensin $\geq$3.5 μg/ml, and polybrene $\geq$25 μg/ml) were used, $P < 0.05$ or even less, indicating the inhibition of remnant binding by these drugs. The dose response of these drugs is summarized in **Table 3**.

Effects of membrane transport blockers on the uptake and degradation of remnants

As shown in Fig. 6B and Table 3, binding of fluorescently labeled remnants on cell surface was affected when the cells were pre-treated with the membrane transport blockers monensin, brefeldin A, colchicine, and polybrene, although none was as effective as suramin in blocking remnant binding. Endocytosis and degradation of remnants were also affected by these reagents. The metabolism of remnants can be deduced from the total fluorescent remnants remaining (pixels/cell) in the cells after prolonged incubation of cells with non-labeled remnants. **Figure 7** compares the fluorescently labeled remnants associated with each cell (pixels/cell) in control versus pre-treated cells at various time points after incubation with non-labeled remnants. Initial binding of fluorescent remnants on cell surface is indicated by the number of pixels/cell at 1 min. In control cells, continued incubation with non-labeled remnants reduced the total number of pixels/cell from 3176 to 103, suggesting that most of remnants were internalized and degraded. The total number of pixels/cell increased from 602 to 992 in cells treated with brefeldin A, suggesting that the degradation of remnants was markedly blocked by this drug. The total number of pixels/cell in cells treated with colchicine, monensin, or polybrene was reduced after a 10-min incubation, but the fluorescence levels remained higher in 30- and 50-min incubations when compared with controls. The results indicated that there were different effects on remnant metabolism by the inhibitors. As a whole, fluorescence persisted much more in cells treated with the various drugs indicating that endocytosis or degradation of remnants was inhibited.

The remnants remaining associated with the cell surface in relation to those internalized by individual cells were quantified as the pixel intensity of the fluorescence label on cell surface and intracellularly. **Figures 8A** and **B** compare the mean pixel intensity on the cell surface in relation to the intracellular remnants. In control cells, the mean pixel intensity on the cell surface decreased markedly with time, indicating efficient endocytosis. In contrast, pixel intensity in cells pre-treated with the inhibitors decreased much slower than in control, suggesting that endocytosis of remnants was decreased by the inhibitors.

The intracellular pixel intensity (Fig. 8B) in control cells increased slightly with time after prolonged incubation with non-labeled remnants. The ratio of intracellular pixel intensity to that at the cell surface was 37%. Cells pre-treated with colchicine accumulated more remnants intracellularly (65% of surface), suggesting a defect in the process of degradation. The pixel intensity of intracellular remnants in cells pre-treated with monensin, brefeldin A, and polybrene all accumulated fluorescent remnants intracellularly (60–88% of surface), suggesting that intracellular degradation of remnants was inhibited to some extent in each case.
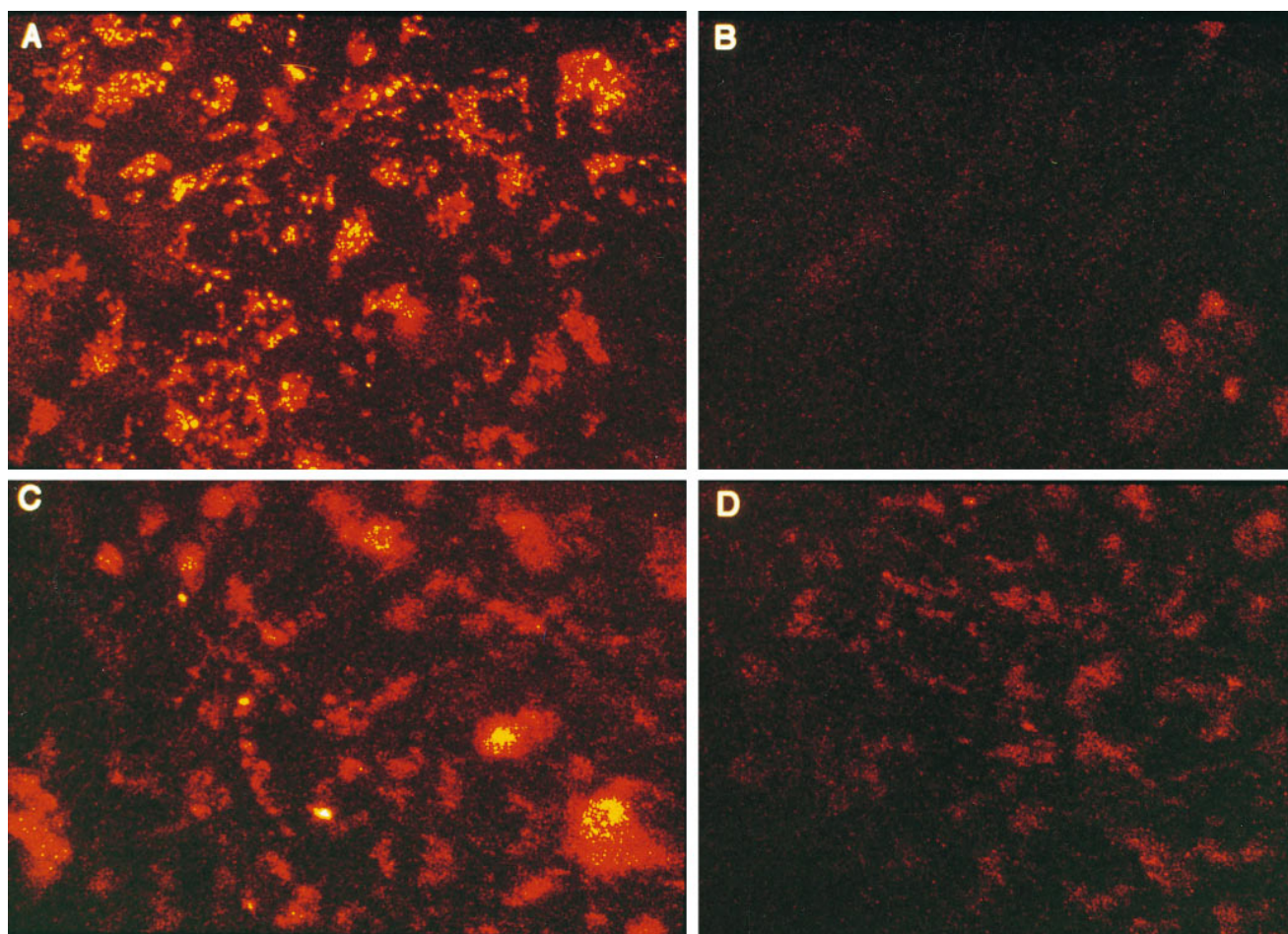
Fig. 5. Effect of antisense and sense ODN transfection on the expression of syndecan in HepG2 cells. (A) Rat anti-syndecan IgG (15 μg/ml/dish) was added to control cells and incubated overnight. Cells were washed, then incubated with FITC-labeled mouse anti rat IgG (30 μg/ml dish) for 2 h. After incubation cells were washed again and then fixed with 4% paraformaldehyde for 1–2 h. (B) As negative control, cells were processed as (A) without the addition of the anti-syndecan IgG. (C) Cells were transfected with sense or (D) antisense oligonucleotides in DOTAP for 24 h, incubated with a rat anti-syndecan antibody overnight and an FITC-labeled mouse anti rat IgG for 2 h, and fixed as in (A).

DISCUSSION

In this study we used a Watson-Crick base-pairing strategy to suppress the expression of syndecan-1 gene in HepG2 cells and studied its effect on remnant binding. Antisense ODNs were used for the sequence-specific inhibition of gene expression. Expression of HSPG was suppressed and remnant binding was decreased in cells transfected with the antisense ODNs. Remnant binding was not totally inhibited probably because heparan sulfates attached to other core proteins of HSPGs also play a role in this process. Surface-bound remnants continued to enter the cells in the presence of antisense ODNs (Fig. 3A) suggesting that once bound, endocytosis of remnants was not dependent on heparan sulfate. When the function of heparan sulfate was completely abolished after treatment with heparinase or suramin, no remnant uptake was observed.

In other studies, high concentrations of ODN have been required due to the poor cellular uptake and rapid intracellular degradation of unmodified ODNs (29). To avoid this problem, cationic lipid (DOTAP) was used to increase the cellular uptake and the phosphodiester (ODNs) were modified to form phosphorothioate ODNs, their isoelectronic congeners. The congeners retain aqueous solubility and Watson-Crick base-pair hybridization, but are resistant to degradation by nucleases (30). In designing the antisense ODNs, we have also avoided using a stretch of four contiguous guanosine residues (4G) to eliminate the non-antisense effect reported by Burgess et al. (21).

Recently Guvakova et al. (31) reported that both

TABLE 2. Effects of syndecan and monoclonal LDL receptor antibodies on remnant binding to cells transfected with ODN sense or antisense to syndecan

| | Transfection | |
| | Sense | Anti-sense |
Pre-incubation	Pixel Intensity (pixel/cell)	Pixel Intensity (pixel/cell)
None	2830 ± 47.5	954 ± 19.2
Anti-syndecan antibody	1373 ± 28.9	694 ± 46.0
Anti-LDL receptor antibody	1113 ± 44.2	622 ± 33.3
Both antibodies	1021 ± 36.7	588 ± 32.3

HepG2 cells were incubated with anti-syndecan antibody, monoclonal anti-LDL receptor antibody, or both antibodies at 37°C for 2 h after transfection with ODNs sense or antisense to syndecan, followed by remnant-like emulsion binding at 4°C as described in the Methods section. Binding was measured by quantitative confocal microscopy and expressed as pixels/cell. Values are means ± SEM of three determinations. Multifactorial analysis of variance showed highly significant effects due to the antisense transfection and to each antibody ($P < 0.001$ in all cases).

phosphodiester ODN and phosphorothioate ODN bind basic fibroblast growth factor, other growth factors, and other heparin-binding molecules. It is thus not unreasonable to predict that decreased remnant binding may occur due to interference by the polyanionic ODN with heparan sulfate, as was the case with suramin. In our study the ODNs were complexed with the cationic liposomes and the charges were presumably shielded from competing with heparan sulfate. Moreover, an anionic polynucleotide, polyinosinic acid, did not affect the binding or uptake of remnants in McA-RH 7777 cells. Furthermore, incorporation of $^{35}SO_4$ into cell surface sulfated compounds was reduced to 78% of control values in cells incubated with the antisense ODN SYN5. The decrease of $^{35}SO_4$ incorporation caused by the antisense ODN was not as marked as the decrease in remnant binding probably because sulfated compounds other than heparan sulfate were present and active on the cell surface. In contrast, no difference was observed in the incorporation of intracellular sulfated compounds, consistent with incorporation of sulfate into the glycosaminoglycan chains on the cell surface (22).

To differentiate whether the decrease in remnant binding was consequent on core protein directly or indirectly through fewer heparan sulfate chains as a result of reduced attachment sites, binding studies were performed in cells pre-treated with competitors, inhibitors, and enzymes that disrupt the function of heparan sulfate without affecting the core protein. Remnant binding was inhibited in cells pre-incubated with a monoclonal antibody to heparan sulfate, or with heparinase, whereas the effect produced by heparitinase I was relatively small. Monoclonal anti-heparan sulfate,

10E4, reacts with an epitope that occurs in native heparan sulfate chains and that is destroyed by N-desulfation of the glycosaminoglycan. The antibody does not react with hyaluronate, chondroitin sulfate, or DNA, and reacts only poorly with heparin (32). Heparinase catalyzes the cleavage of iduronic acid-containing disaccharide linkages where the glucosamine is sulfated at the 2-position. These linkages are conspicuously present in HSPG and appear to play the major role in remnant binding. Heparitinase I only acts specifically on heparan sulfate regions containing the α-1,4-N-acetyl-d-glucosamine linkage, where the glucosamine is not sulfated at the 6-position (27). Remnant binding decreased by 23% when these linkages were cleaved by heparitinase I, suggesting that these linkages contribute to remnant binding to some extent.

Xyloside and its derivatives have been shown to inhibit HSPG synthesis in bovine corneal endothelial cells (33), in SV40 transformed Swiss Mouse 3T3 cells (34), in cultured rabbit granulosa cells (28), in embryonic chick cornea (35), and in glomerular basement membranes (36) of rats. In these systems, xylosides have been demonstrated to act by providing a primer for glycosaminoglycan (GAG), thus stimulating the synthesis of free GAG chains. The xyloside-initiated chains are not retained in the extracellular matrices and are discharged rapidly into the medium (28, 36). Xyloside competes with the native acceptor for the initiation of synthesis of heparan sulfate chains on the protein core and inhibits the synthesis of proteoglycan. As a result, the protein core of cell surface HSPG contains fewer GAG chains, which could decrease remnant binding. A structural analogue of xyloside, β-d-galactoside had no effect on proteoglycan synthesis, although increasing GAG synthesis to a lower degree (28, 37). Our findings show that remnant binding was reduced in the presence of 4-nitrophenyl-β-d-xylopyranoside whereas 4-nitrophenyl-β-d-galactopyranoside, which did not compete for the initiation site with xylose, had no effect on remnant binding. These findings confirm the involvement of heparan sulfate rather than the core protein of HSPG in remnant binding.

Beisiegel et al. (38) have shown that the monoclonal antibody to the LDL receptor reacts with the human and bovine LDL receptor, but not with receptor from the mouse, rat, Chinese hamster, rabbit, or dog. In this study, remnant binding was reduced by about 61% in cells treated with the monoclonal anti-LDL receptor IgG. Residual binding shows there was an LDL receptor-independent pathway. This finding was consistent with our previous in vivo results (3). The remnant binding was reduced by 51% in cells treated with anti-syndecan IgG. The binding was decreased even more when the cells were transfected with antisense and/or incubated
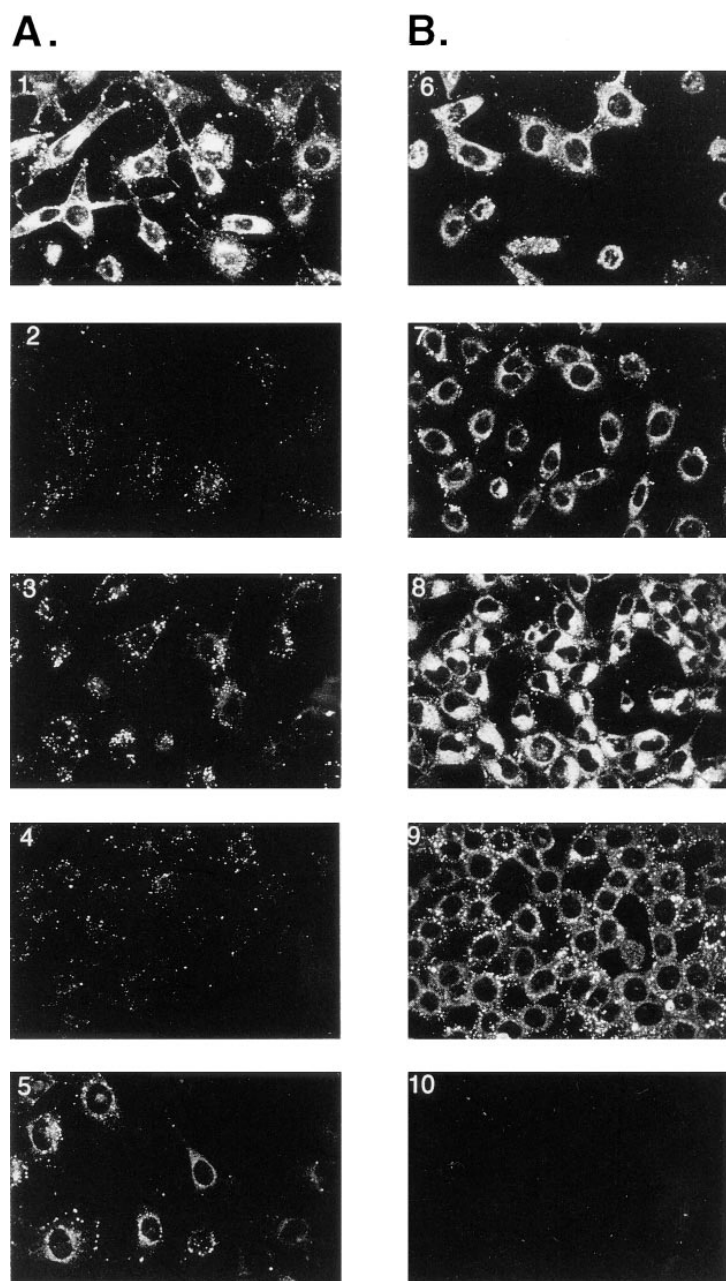
Fig. 6. Binding and uptake of fluorescently labeled chylomicron remnants by cells pretreated with reagents to degrade heparan sulfate or disrupt the function of heparan sulfate. (A) Cells were incubated at 37°C for 24 h with (1) medium only, (2) 1 unit/ml of heparinase, (3) 0.5 units/ml heparitinase, (4) 4 ng/ml anti-heparan sulfate antibody, and for 48 h with (5) 4-NP-xylopyranoside (1 mm). After incubation with the reagents, cells were washed and incubated immediately with cholesteryl-BODIPY labeled remnants for 5 min and then re-equilibrated with a similar amount of non-labeled remnants for 1 min. In the case of the antibody, cells were incubated with fresh medium at 37° for 2 h to reduce non-specific binding before remnants were added. The cells were then fixed in 4% paraformaldehyde and processed for confocal microscopy. Figures show the results obtained from HepG2 cells. Similar results were observed in McA-RH7777 cells. (B) HepG2 cells were incubated at 37°C for 1 h with solutions (final concentration) containing (6) colchicine (400 μg/ml), (7) BFA (10 μg/ml), (8) monensin (20 μm or 14 μg/ml), (9), polybrene (12.5 μg/ml), and (10) suramin (500 μg/ml) or any of the three polypeptides at 320 μg/ml, before treatment with fluorescently labeled remnants and non-labeled remnants as described in (A).

with both anti-syndecan IgG and anti-LDL receptor IgG. Our results showed that the binding of remnants was dependent on both the LDL receptor and the function of HSPG.

Herz et al. (39) described the LDL receptor-related protein (LRP) as a multifunctional receptor expressed in a variety of cell types. It has been shown to be a multiligand receptor for lipoprotein remnants and other physiologically important ligands, mediating cellular uptake of apoE-containing, remnant-like lipoproteins (reviewed in ref. 40). The relationship between LRP and HSPG is still unknown, but it is possible that

HSPGs on the cell surface serve as the initial binding site for the remnants with apoE and then present the remnants to LRP and other possible receptors for endocytosis by the cells.

The structure of heparan sulfate in the liver is unique because of its high sulfate content (41). Lyon, Deakin, and Gallagher (41) showed that the combination of high N- and O-sulfation in HSPG translated to a total sulfate content of 1.34 sulfates/disaccharide, which was 50% higher than most heparan sulfate species. A high level of sulfation of heparan sulfate is required for protein binding (41). Consistent with this

TABLE 3. Effects of membrane transport inhibitors on remnant binding

Cells Pre-treated with Inhibitors

A. Colchicine							
Concentrations (μg/ml)	0	4	40	100	200	400	600
Remnants bound (pixels/cell)	2288 ± 112.3	1750 ± 404.8	1177 ± 169.1	1885 ± 435.4	2127 ± 208.3	1408 ± 192.6	1221 ± 16.7
B. Brefeldin A							
Concentrations (μg/ml)	0	1.0	2.5	5.0	10	20	
Remnants bound (pixels/cell)	2498 ± 224.9	2866 ± 78.7	1817 ± 51.3	1364 ± 172.9	507 ± 98.8	70.51 ± 18.2	
C. Monensin							
Concentrations (μg/ml)	0	0.7	3.5	7.0	14	21	28
Remnants bound (pixels/cell)	2627 ± 130.3	2096 ± 219.4	1220 ± 52.6	1657 ± 230.5	1458 ± 137.2	1304 ± 56.9	1519 ± 61.7
D. Polybrene							
Concentrations (μg/ml)	0	12.5	25	50	100	150	
Remnants bound (pixels/cell)	2020 ± 76.5	1818 ± 104.2	825 ± 116.1	676 ± 109.1	1241 ± 95.6	850 ± 52.9	

HepG2 cells plated and grown on coverslips in 35-mm plastic culture dishes were treated with membrane transport blockers followed by remnant binding and uptake studies as described in Methods. Binding and uptake of remnants were measured by quantitative confocal microscopy. Initial binding of remnants to cell surface was shown by the number of pixels/cell after incubation of cells with fluorescent remnants for 5 min and re-equilibrated with non-labeled remnants for 1 min. Values are means ± SEM of three different determinations.

argument, our results show that suramin, a highly sulfated molecule, could totally abolish remnant metabolism by liver cells in mice (3) and in tissue culture, probably by competing with heparan sulfate for the binding of remnants. Fucoidan, another sulfated polysaccharide, also effectively reduced the binding of remnants to cell surface.

Positively charged polypeptides including poly-arginine, poly-lysine, and protamine also inhibited remnant binding. The mechanism is unclear but is probably due to the interaction of the cations with the negatively charged heparan sulfate chains. A synthetic polycation,

polybrene (hexadimethrine bromide) also inhibited the binding and internalization of remnants by cells (Fig. 7) indicating that binding must involve cation–anion attractions. Polybrene also inhibited the degradation of remnants after endocytosis, as indicated by the accumulation of intracellular fluorescently labeled remnants after prolonged incubation with non-labeled remnants.

Membrane transport inhibitors, such as monensin, colchicine, and brefeldin A, reduced remnant binding to some extent but effectively inhibited remnant degradation after internalization. Monensin is a monovalent cation ionophore that exchanges monovalent ions in-
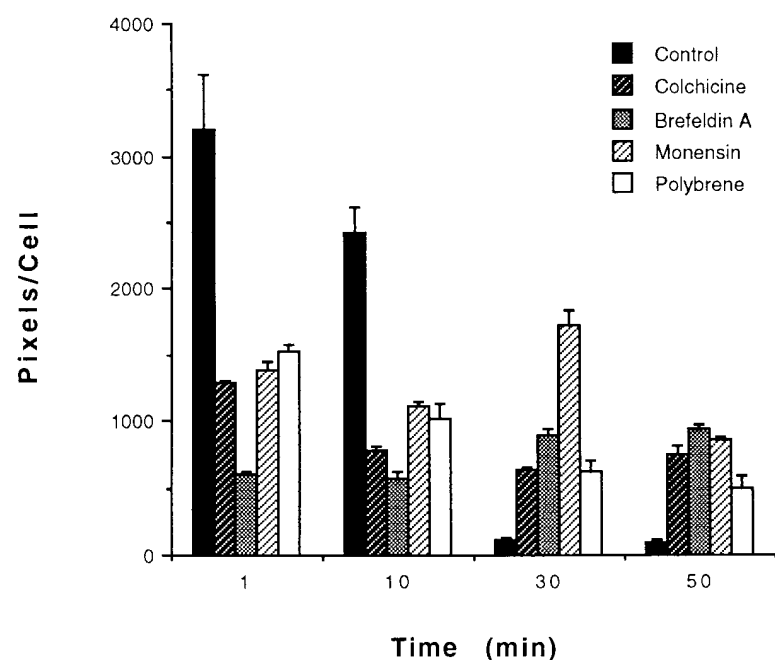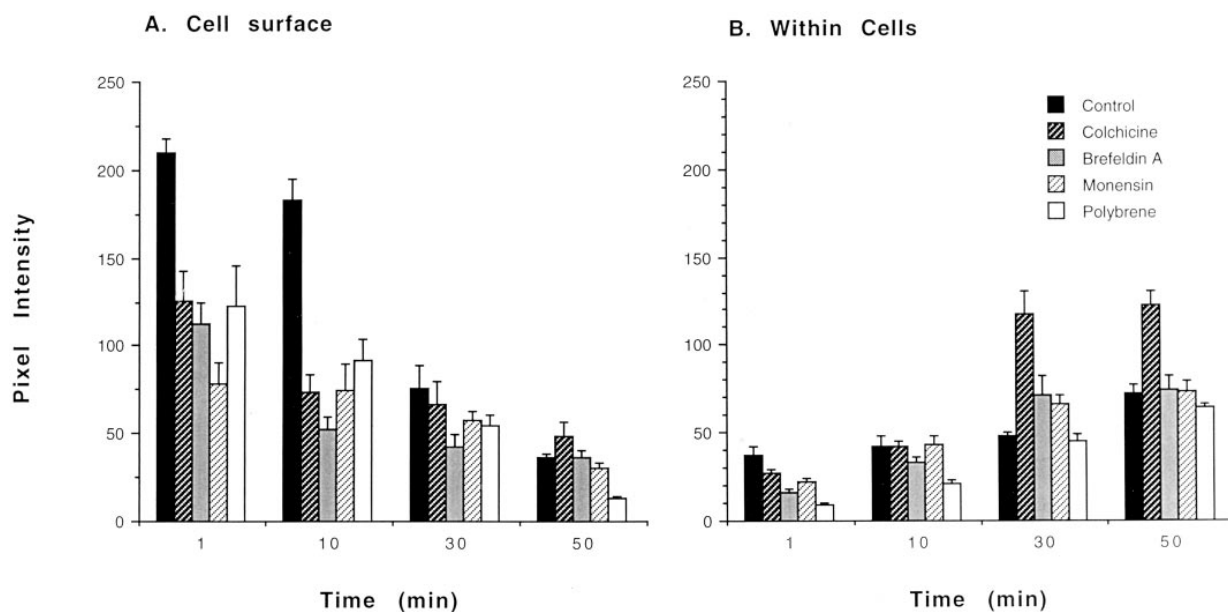

Fig. 7. Effect of membrane transport blockers and metabolic inhibitors on the uptake and metabolism of remnants. HepG2 cells were pretreated with (i) medium only, (ii) colchicine (400 μg/ml), (iii) BFA (10 μg/ml), (iv) monensin (20 μM or 14 μg/ml), (v), polybrene (12.5 μg/ml), incubated with fluorescently labeled remnants, and reequilibrated with non-labeled remnants for 1, 10, 30, and 50 min. The fluorescently labeled remnants associated with cells (surface and intracellular) were quantified as number of pixels/cell. Initial binding of fluorescently labeled remnants is indicated by pixels/cell at 1 min; continued incubation with non-labeled remnants reduced the total number of pixels/cell, suggesting that remnants were internalized and degraded in control cells but not in cells pre-treated with inhibitors. Values are means ± SEM of three different determinations.

A. Cell surface

B. Within Cells

Control
Colchicine
Brefeldin A
Monensin
Polybrene

Fig. 8. Effect of membrane transport blockers and metabolic inhibitors on the surface and intracellular remnants. HepG2 cells were treated as in Fig. 7. The fluorescently labeled remnants remaining associated with the cell surface in relation to those inside individual cells were quantified as the pixel intensity of the fluorescent label on the cell surface (A) and intracellularly (B). Values are means ± SEM of three different determinations.

cluding protons. It disrupts a proton gradient maintained by an ATP-dependent proton pump believed to be present in Golgi membranes, causing a rise in the pH of the Golgi sub-compartments. Monensin has been shown to slow intra-Golgi transport, inhibit late Golgi functions, and perturb endocytic traffic and plasma-lemmal receptor recycling (42–44). Monensin has also been reported to inhibit the synthesis of glycosaminoglycans on proteoglycan molecules (45). As shown in Fig. 7, endocytosis and degradation of remnants were inhibited by monensin, consistent with previous findings (46). The disruption of remnant metabolism by monensin could be twofold. First, via the reduction of heparan sulfate synthesis and second, by alteration of the normal Golgi function and disruption of the events involved in endocytosis. However, in the present study the incubation time of monensin in cells was probably not sufficient to inhibit heparan synthesis. A similar interpretation probably explains the inhibition of remnant uptake by BFA (Table 3). Furthermore, colchicine inhibited the degradation of remnants suggesting that the functional integrity of microtubules is important in the process of endocytosis and degradation of remnants.

In conclusion, our results show that suppression of syndecan expression decreases remnant binding in liver cells, possibly secondary to decreased expression of cell surface heparan sulfate chains, as several lines of experimental evidence support a role for heparan sulfate in remnant binding. Our data confirm that the LDL receptor is important in the binding of remnant-like emulsions to HepG2 cells.

REFERENCES

1. Liao, W. 1995. β-Migrating very low density lipoprotein, chylomicron remnants and their receptors. *Biochem. J.* **310:** 359. (Comment)
2. van Berkel, T. J. C., A. Voorschuur, and J. Kuiper. 1995. β-Migrating very low density lipoproteins and chylomicron remnants bind to rat liver hepatocytes at a low-density-lipoprotein-independent site (the remnant receptor). *Biochem. J.* **310:** 359–360. (Letter)
3. Mortimer, B-C., D. J. Beveridge, I. J. Martins, and T. G. Redgrave. 1995. Intracellular localization and metabolism of chylomicron remnants in the livers of LDL receptor-deficient mice and apoE-deficient mice. Evidence for slow metabolism via an alternative apoE-dependent pathway. *J. Biol. Chem.* **270:** 28767–28776.
4. Kita, T., J. L. Goldstein, M. S. Brown, Y. Watanabe, C. A. Hornick, and R. J. Havel. 1982. Hepatic uptake of chylo-

micron remnants in WHHL rabbits: a mechanism genetically distinct from the low density lipoprotein receptor. *Proc. Natl. Acad. Sci. USA.* **79:** 3623–3627.

5. Rubinsztein, D. C., J. C. Cohen, G. M. Berger, D. R. van der Westhuyzen, G. A. Coetzee, and W. Gevers. 1990. Chylomicron remnant clearance from the plasma is normal in familial hypercholesterolemic homozygotes with defined receptor defects. *J. Clin. Invest.* **86:** 1306–1312.

6. Windler, E., J. Greeve, B. Levkau, V. Kolb-Bachofen, W. Daerr, and H. Greten. 1991. The human asialoglycoprotein receptor is a possible binding site for low-density lipoproteins and chylomicron remnants. *Biochem. J.* **276:** 79–87.

7. Yen, F. T., C. J. Mann, L. M. Guermani, N. F. Hannouche, N. Hubert, C. A. Hornick, V. N. Bordeau, G. Agnani, and B. E. Bihain. 1994. Identification of a lipolysis-stimulated receptor that is distinct from the LDL receptor and the LDL receptor-related protein. *Biochemistry.* **33:** 1172–1180.

8. Huettinger, M., H. Retzek, M. Hermann, and H. Goldenberg. 1992. Lactoferrin specifically inhibits endocytosis of chylomicron remnants but not alpha-macroglobulin. *J. Biol. Chem.* **267:** 18551–18557.

9. Ji, Z. S., and R. W. Mahley. 1994. Lactoferrin binding to heparan sulfate proteoglycans and the LDL receptor-related protein—further evidence supporting the importance of direct binding of remnant lipoproteins to HSPG. *Arterioscler. Thromb.* **14:** 2025–2031.

10. Ji, Z. S., W. J. Brecht, R. D. Miranda, M. M. Hussain, T. L. Innerarity, and R. W. Mahley. 1993. Role of heparan sulfate proteoglycans in the binding and uptake of apolipoprotein E-enriched remnant lipoproteins by cultured cells. *J. Biol. Chem.* **268:** 10160–10167.

11. Ji, Z. S., D. A. Sanan, and R. W. Mahley. 1995. Intravenous heparinase inhibits remnant lipoprotein clearance from the plasma and uptake by the liver: in vivo role of heparan sulfate proteoglycans. *J. Lipid Res.* **36:** 583–592.

12. Mahley, R. W., Z-S. Ji, W. J. Brecht, R. D. Miranda, and D-P. He. 1994. Role of heparan sulfate proteoglycan and the LDL receptor-related protein in remnant lipoprotein metabolism. *Ann. NY Acad. Sci.* **737:** 39–52.

13. Ji, Z. S., S. Fazio, Y. L. Lee, and R. W. Mahley. 1994. Secretion-capture role for apolipoprotein-E in remnant lipoprotein metabolism involving cell surface heparan sulfate proteoglycans. *J. Biol. Chem.* **269:** 2764–2772.

14. Andres, J., D. DeFalcis, and J. Massague. 1992. Binding of two growth factor families to separate domains of the proteoglycan betaglycan. *J. Biol. Chem.* **267:** 5927–5930.

15. Roskams, T., H. Moshage, R. De Vos, D. Guido, P. Yap, and V. Desmet. 1995. Heparan sulfate proteoglycan expression in normal human liver. *Hepatology.* **21:** 950–958.

16. Rapraeger, A., M. Jalkanen, E. Endo, J. Koda, and M. Bernfield. 1985. The cell surface proteoglycan from mouse mammary epithelial cells bears chondroitin sulfate and heparan sulfate glycosaminoglycans. *J. Biol. Chem.* **260:** 11046–11052.

17. Mortimer, B. C., W. J. Simmonds, S. J. Cockman, R. V. Stick, and T. G. Redgrave. 1990. The effect of monostearoylglycerol on the metabolism of chylomicron-like lipid emulsions injected intravenously in rats. *Biochim. Biophys. Acta.* **1046:** 46–56.

18. Mortimer, B. C., W. J. Simmonds, C. A. Joll, R. V. Stick, and T. G. Redgrave. 1988. Regulation of the metabolism of lipid emulsion model lipoproteins by a saturated acyl chain at the 2-position of triacylglycerol. *J. Lipid Res.* **29:** 713–720.

19. Martins, I. J., C. Vilcheze, B-C. Mortimer, R. Bittman and T. G. Redgrave. 1998. Sterol side chain length and structure affect the clearance of chylomicron-like lipid emulsions in rats and mice. *J. Lipid Res.* **39:** 302–312.

20. Mali, M., P. Jaakkola, A-M. Arvilommi, and M. Jalkanen. 1990. Sequence of human syndecan indicates a novel gene family of integral membrane proteoglycans. *J. Biol. Chem.* **265:** 6884–6889.

21. Burgess, T. L., E. F. Fisher, S. L. Ross, J. V. Bready, Y-X. Qian, L. A. Bayewitch, A. M. Cohen, C. J. Herrera, S. S-F. Hu, T. B. Kramer, F. D. Lott, F. H. Martin, G. F. Pierce, L. Simonet, and C. L. Farrell. 1995. The antiproliferative activity of c-myb and c-myc antisense oligonucleotides in smooth muscle cells is caused by a nonantisense mechanism. *Proc. Natl. Acad. Sci. USA.* **92:** 4051–4055.

22. Rapraeger, A., and M. Bernfield. 1985. Cell surface proteoglycan of mammary epithelial cells. *J. Biol. Chem.* **260:** 4103–4109.

23. Bartlett, G. R. 1959. Phosphorus assay in column chromatography. *J. Biol. Chem.* **234:** 466–468.

24. Carlson, L. A. 1963. Determination of serum triglyceride. *J. Atheroscler. Res.* **3:** 334–336.

25. Zlatkis, A., and B. Zak. 1969. Study of a new cholesterol reagent. *Anal. Biochem.* **29:** 143–148.

26. Lowry, O. H., N. J. Rosebrough, A. L. Farr, and R. J. Randall. 1951. Protein measurements with Folin phenol reagent. *J. Biol. Chem.* **193:** 265–275.

27. Nader, H. B., C. P. Dietrich, V. Buonassisi, and P. Colburn. 1987. Heparin sequences in the heparan sulfate chains of an endothelial cell proteoglycan. *Proc. Natl. Acad. Sci. USA.* **84:** 3565–3569.

28. Benhaim, A., C. Feral, M. Langris, J. Bocquet, and P. Leymarie. 1995. Progesterone secretion and proliferation in cultured rabbit granulosa cells under conditions of β-d-xyloside-induced inhibition of proteoglycan synthesis. *Biol. Reprod.* **52:** 939–946.

29. Gura, T. 1995. Antisense has growing pains. *Science.* **270:** 575–577.

30. Stein, C. A., C. Subasinghe, K. Shinozuka, and J. S. Cohen. 1988. Physicochemical properties of phosphorothioate oligonucleotides. *Nucleic Acids Res.* **16:** 3209–3221.

31. Guvakova, M. A., L. A. Yakubov, I. Vlodavsky, J. L. Tonkinson, and C. A. Stein. 1995. Phosphorothioate oligodeoxynucleotides bind to basic fibroblast growth factor, inhibiting its binding to cell surface receptors, and remove it from low affinity binding sites on extracellular matrix. *J. Biol. Chem.* **270:** 2620–2627.

32. David, G., X. M. Bai, B. Van der Schueren, J-J. Cassiman, and H. Van der Berghe. 1992. Developmental changes in heparan sulfate expression: in situ detection with mAbs. *J. Cell Biol.* **119:** 961–975.

33. Robinson, J., and D. Gospodarowicz. 1984. Effect of *p*-nitrophenyl-β-d-xyloside on proteoglycan synthesis and extracellular matrix formation by bovine corneal endothelial cell cultures. *J. Biol. Chem.* **259:** 3818–3824.

34. Johnston, L. S., and J. M. Keller. 1979. The effect of β-xylosides on heparan sulfate synthesis by SV40-transformed Swiss Mouse 3T3 cells. *J. Biol. Chem.* **254:** 2575–2578.

35. Hart, G. W., and W. Lennarz. 1978. Effects of tunicamycin on the biosynthesis of glycosaminoglycans by embryonic chick cornea. *J. Biol. Chem.* **253:** 5795–5801.

36. Kanwar, Y. S., V. C. Hascall, M. L. Jakubowski, and J. T. Gibbons. 1984. Effects of β-d-xyloside on the glomerular

proteoglycans. I. Biochemical studies. *J. Cell Biol.* **99:** 715–722.

37. Phamantu, N. T., P. J. Bonnamy, M. Bouakka, and J. Bocquet. 1995. Inhibition of proteoglycan synthesis induces an increase in follicle stimulating hormone (FSH)-stimulated estradiol production by immature rat Sertoli cell. *Mol. Cell Endocrinol.* **109:** 37–45.

38. Beisiegel, U., W. J. Schneider, J. L. Goldstein, R. G. W. Anderson, and M. S. Brown. 1981. Monoclonal antibodies to the low density lipoprotein receptor as probes for study of receptor-mediated endocytosis and the genetics of familial hypercholesterolemia. *J. Biol. Chem.* **256:** 11923–11931.

39. Herz, J., U. Hamann, S. Rogne, O. Myklebost, H. Gausepohl, and K. K. Stanley. 1988. Surface location and high affinity for calcium of a 500-kD liver membrane protein closely related to the LDL-receptor suggest a physiological role as lipoprotein receptor. *EMBO J.* **7:** 4119–4127.

40. Krieger, M., and J. Herz. 1994. Structures and functions of multiligand lipoprotein receptors: macrophage scavenger receptors and LDL receptor-related protein (LRP). *Annu. Rev. Biochem.* **63:** 601–637.

41. Lyon, M., J. A. Deakin, and J. T. Gallagher. 1994. Liver heparan sulfate structure. *J. Biol. Chem.* **269:** 11208–11215.

42. Brown, M. S., R. G. W. Anderson, and J. L. Goldstein. 1983. Recycling receptors: the round-trip itinerary of migrant membrane proteins. *Cell.* **32:** 663–667.

43. Wilcox, D. K., R. P. Kitson, and C. C. Widnell. 1982. Inhibition of pinocytosis in rats embryo fibroblast treated with monensin. *J. Cell Biol.* **92:** 859–864.

44. Wileman, T., R. L. Boshans, P. Schlesinger, and P. Stahl. 1984. Monensin inhibits recycling of macrophage mannose-glycoprotein receptors and ligand delivery to lysosomes. *Biochem. J.* **220:** 665–675.

45. Yanagishita, M., and V. C. Hascall. 1985. Effects of monensin on the synthesis, transport, and intracellular degradation of proteoglycans in rat ovarian cells in culture. *J. Biol. Chem.* **260:** 5445–5455.

46. Basu, S. K., J. L. Goldstein, R. G. W. Anderson, and M. S. Brown. 1981. Monensin interrupts the recycling of low density lipoprotein receptors in human fibroblasts. *Cell.* **24:** 493–502.